Eur. Phys. J. Plus (2023) 138:644
https://doi.org/10.1140/epjp/s13360-023-04187-8

THE EUROPEAN PHYSICAL JOURNAL PLUS

Regular Article

Examination of gecko-inspired dry adhesives for heritage conservation as an example of iterative design and testing process for new adhesives

Jacek Olender[1,2,a], **Christina Young**[1,b]

[1] Kelvin Centre for Conservation and Cultural Heritage Research, College of Arts, University of Glasgow, Glasgow, UK
[2] Image Permanence Institute, Rochester Institute of Technology, Rochester, NY, USA

Received: 15 October 2022 / Accepted: 10 June 2023

Abstract Rarely within the conservation of cultural heritage have conservation professionals been lucky enough to have materials custom-designed to meet their requirements. Most of the time the field must adapt solutions developed for other applications. The research presented here was initiated as part of a long-term aim to develop new adhesives for heritage conservation. Gecko-inspired dry adhesives (GDAs) are polymer tapes with micropatterns that are based on the adhesive properties of the pads of gecko lizard feet: they have strong normal and shear adhesion with low peel adhesion. They present potentially versatile and reversible adhesives for heritage conservation applications; which do not require solvents for activation or for removal, and do not migrate or off-gas. In nature, geckos can adhere with their feet to any surface they walk on. This is possible because of micro- and nanostructures on their feet that attach to surface via van der Waals forces. Practical studies aimed at comprehensively assessing their properties, and biomimetic solutions in heritage conservation are still sparse at present. This research has the objective of assessing GDAs properties by mechanical testing of adhesive joints, as well as physical and chemical characterisation of the materials used. The research has also included a museum case study and a two-year natural ageing test. The testing has shown that the GDAs can perform very well as an adhesive patch on the reverse of gelatine-based photographs, achieving shear forces between 0.80 N and 48.10 N on 8 cm^2 lap joints (depending on the type of the GDA) and peel forces between 0.20 N and 0.47 N over 2 cm of peel front. This is lower than forces exceeding 1 N recorded in widely available pressure-sensitive tapes. This shows that GDAs may have the potential of a sufficiently strong, yet easily removable adhesive that works well on materials widely present in museum collections.

1 Introduction

1.1 Principles of adhesive design and protocol for conservation adaptation

Gecko-inspired dry adhesives (GDAs) are a biomimetic solution. Meaning that a phenomenon observed in nature is deemed an interesting engineering solution and designs have been developed into prototypes that follow the same working principles providing at least some of the properties of the naturally occurring phenomenon [1–4]. It may be argued that conservation and biomimetics are complementary disciplines because one is a discipline in constant need of solutions, while the other is a discipline in constant search for applications. To date, the use of GDAs has been investigated empirically for their applicability for use with objects of cultural heritage and a safe application [5, 6].

Adhesives are one of the essential materials of heritage conservation. They are omnipresent in heritage material and a necessary part many conservation treatments which require structural intervention. Adhesives are applied both as temporary (facings, fixings, and exhibition mounts) and permanent (consolidation and reattachment) solutions [7]. As such, they must fulfil not only the technical requirements for the effectiveness of their application, but also several ethical considerations [8, 9]. Both are crucial factors in developing assessment and testing protocol before introducing new adhesives into the field of conservation.

An iterative design flow chart is proposed (see Fig. 1); using our GDA research as an example we discuss its application. The flow chart has eight key points, which can be used from a conservation perspective (i.e. problem at hand) and biomimetic perspective (i.e. material with potential applications). In the points below, the adhesion of the "material-adhesive" systems is discussed, and by "material" the heritage material being treated is described. Adhesives are used as an example, but the iterative design process can be successfully applied to other treatment solutions.

[a] emails: jacek.olender@glasgow.ac.uk; jacek.olender@rit.edu (corresponding author)
[b] e-mail: christina.young@glasgow.ac.uk

Published online: 24 July 2023

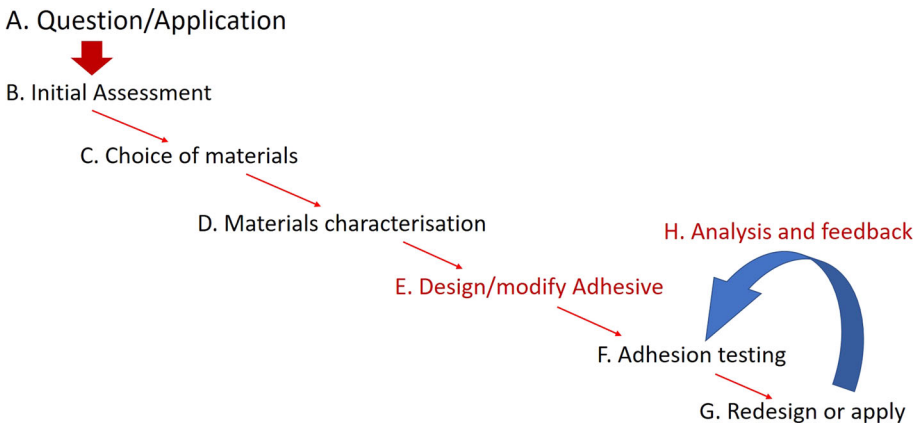

Fig. 1 A work flow chart for the proposed testing protocol for introducing new adhesives in heritage conservation

A Question or application:

- What is the nature of the adhesion problem?
- What are the promising properties of the new adhesive?

B Initial assessment:

- Are there any potential solutions that have not been tested before?
- What materials can the new adhesive be used on, based on its known properties?

C Choice of materials:

- What new materials have the best chances of succeeding?
- What materials are the best suited for the application of a new solution?

D Materials characterisation:

- What are the relevant basic properties of the materials chosen for investigation that will determine successful outcome?

E Design/modify:

- Are there changes that need to be made in the material of choice to ensure the success of future application?

F Adhesion testing:

- What tests can be conducted on the material-adhesive pairing that will provide the necessary information for the final method assessment?

G Redesign or application:

- If the material-adhesive pairing fails to perform as desired, what changes could be made to improve the design?
- If the material performs well–can it be now applied?

H Feedback:

- Is the material-adhesive system working well or failing?
- Did the tests conducted provide all the necessary information for correct assessment?
- If not, what changes should be made to the adhesive and the testing methodology?

This simple protocol can serve as handy checklist for researchers and conservators alike.

2 The principles of gecko adhesion

In order to introduce a biomimetic adhesive into conservation practice, the principles of its adhesion mechanism need to be understood and assumptions have to be made on how it can be put to work (Point A of the protocol). Gecko-inspired dry adhesives (GDAs) are materials that are created to mimic adhesive properties of pads found on the undersides of gecko feet. Geckos are group of lizard species recognized for their ability to stick to any surface, vertical or even upside down, without an adhesive chemically interacting with the surface. This ability has raised questions and interest since ancient Greece [10], but the mechanism was not understood until 2000, when Autumn et al. [11] explained it in their seminal paper. Geckos can walk as they do because of rows of micro-hairs on

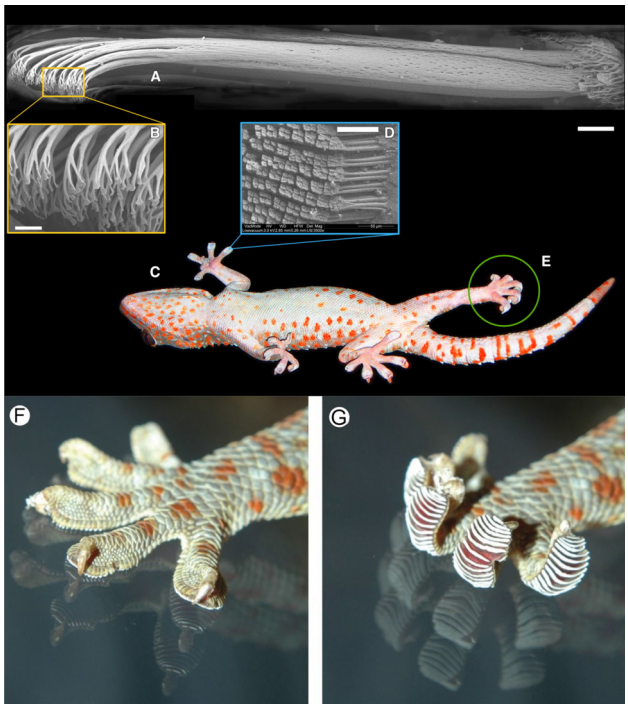

Fig. 2 Details of gecko locomotion system. **A** single seta micro-hair; **B** spatulae tips; **C** attached gecko; **D** rows of setae; **E** detached gecko foot; **F** attached gecko foot showing the digits pressed against the surface; **G** gecko foot during detachment, showing rolling back of geckos's digits for the ease of removal. Scalebars: A = 5 μm, B = 1 μm, D = 50 μm. **A**–**E**: Image by Gorb and Autumn, reproduced with permission from [13]. **F**–**G**: Image reproduced and edited with permission, from [18]. Not included in CC license, copyright lies with the respective journals and authors

their feet called setae. Setae are between 30 and 130 μm long and approx. 2 μm thick.[1] Each one of them branches into hundreds of spatulae–thinner, few microns long hairs with spatula-shaped tips. Each such tip is approximately 150 nm wide and 5 nm thick [12], as can be seen in Fig. 2A–D. The adhesive attraction between the spatulae and the surface on which a gecko walks occurs through the van der Waals secondary bonding forces [11, 13], with probable influence of capillary [14, 15] and electrostatic forces [16]. The presence of these other phenomena is probably contingent on the environment in which the lizard happens to find itself. However, assuming ideal conditions with all the spatulae perfectly attached to the surface, a gecko would stick with a normal adhesion force exceeding its weight by at least 100 times [17, 18]. At the same time, geckos run away from predators because they can detach their feet very easily. They do this by rolling back their toes, a process that breaks the connection of one micro-hair at a time. Therefore, they detach feet via this peeling process, and resulting force is a fraction of the shear or normal adhesion of the entire pad. This digit roll-back process is illustrated in Fig. 2E–G.

This mechanism inspired engineers to create artificial adhesive gecko pads as soon as its principles were understood. The first attempts at creating GDAs were made almost immediately after the Autumn et al. paper, who had themselves already speculated about a possibility of creating synthetic gecko pads [19, 20]. Such efforts have significantly expanded in the last few years [21]. The application potential of the GDAs was noticed by the conservation community, and in 2011 Julia Fenn from the Canadian Conservation Institute presented a paper in which she suggested adapting GDAs for conservation practice [22]. Preliminary assessment of GDAs used in conservation came with the early results of this present research (testing only one type of GDA) [23] and the work by Izadi et al. [24] who tested a fibrillar adhesive for its ability of removing dirt particles from fragile surfaces.

GDAs offer potential solutions for some treatment and museum procedures in which physical immobilisation of an object, or its parts is necessary. GDAs do not require solvents or any chemical interaction with the substrate surface in order to adhere to it. They also provide immediate maximum adhesion with minimal preload, which is strong in normal and shear directions, but with relatively low peel. Therefore, GDAs can potentially make a temporary patch, a securing layer for transport, as a facing, or immobilisation of an object during a conservation treatment or in a showcase.

This research is aimed at assessing such applications using data from application of commercially available GDAs and of prototypes developed in-house. Multiple testing set-ups for the GDAs, each in a set range of environmental conditions, are investigated.

[1] Data of the gecko anatomy presented are for the Tokay Gecko (*Gekko gecko*), the largest and probably the most-studied of the adhering gecko species.

Table 1 List of tests conducted in this research, sorted according to the environmental conditions

Tests conducted		Relative Humidity		
Temp		33%	55%	75%
	5 °C	Tensile of PH	Tensile of PH, GB2 & GB3	Tensile of PH
		Shear & Peel of GB2 GDA on PH	Shear & Peel of GB2 GDA on PH	Shear & Peel of GB2 GDA on PH
		Shear & Peel of GB3 GDA on PH	Shear & Peel of GB2 GDA on PH	Shear & Peel of GB3 GDA on PH
	21 °C	Tensile of PH & GB1	Tensile of PH, GB2 & GB3	Tensile of PH
		Shear & Peel of GB1 GDA on PH	Shear & Peel of GB2 GDA on PH	Shear & Peel of GB2 GDA on PH
		Shear & Peel of GB2 GDA on PH	Shear & Peel of GB2 GDA on PH	Shear & Peel of GB3 GDA on PH
		Shear & Peel of GB3 GDA on PH	Stress relaxation of GB2	
			Stress relaxation of GB3	
			Peeling of PSA tapes (TSELL & TARC)	
	35 °C	Tensile of PH	Tensile of PH, GB2 & GB3	Tensile of PH
		Shear & Peel of GB2 GDA on PH	Shear & Peel of GB2 GDA on PH	Shear & Peel of GB2 GDA on PH
		Shear & Peel of GB3 GDA on PH	Shear & Peel of GB2 GDA on PH	Shear & Peel of GB3 GDA on PH

Codes: PH–photographic prints, GB1 & GB2–two versions of commercial GDAs with a PSA backing, GB3–a commercial GDA without backing, UOG–custom-made GDA, TSELL–Sellotape ®, TARC – Archival tape

3 Materials and methods

Initially, a wide range of GDAs was considered[2] (as suggested in point B of the flow chart). This was narrowed to three types of GDAs manufactured by the Gottlieb Binder GmbH and two prototypes prepared by the team at the James Watt Nanofabrication Centre at the University of Glasgow. To find an applicable testing substrate and to devise a systematic testing protocol (cf. point C) the GDAs selected were initially tested on a range of substrate materials. These materials included: stainless steel, wood (coated and not coated), poly(methyl methacrylate), copper and variety of coated papers. The collection was diverse, based on samples easily available at the time. The basic properties of the surfaces were recorded including electrostatic characteristics or roughness (judged by eye). Among the coated papers, photographic prints were eventually selected as the substrate material to test the GDAs. They were chosen for their ease of acquisition and testing and after consultations with professionals researching and conserving photographic prints [23] as having the greatest potential as a useful GDA application. A range of tests were conducted on the substrate materials and on the GDAs to identify their physical and chemical properties before testing adhesive properties (cf. point D). GDAs were examined using all of the methods listed below. The photographic prints were not examined with DMA or stress relaxation testing because the potential results were not deemed informative.

1. Optical Microscopy
2. Fourier Transform Infrared Spectroscopy–Attenuated Total Reflectance (FTIR-ATR)
3. Environmental Scanning Electron Microscope (ESEM)
4. Dynamic Mechanical Analysis (DMA)
5. Tensile testing
6. Stress relaxation testing

In this design of a new adhesive (point E) was not necessary, since several GDAs were available. Therefore, testing of adhesive joints could proceed (point F). Mechanical testing of adhesive joints was conducted in shear and peel configurations, with peeling set in a T-Peel arrangement, widely used methods for characterisation of adhesives [25–27]. The mechanical tests of both joints and individual materials were conducted in a range of temperature and relative humidity values (see Table 1). The temperature ranged between 5 °C and 35 °C and the relative humidity ranged between 33% and 75%. However, some materials were not available in later part of the project, as they had been discontinued and could not be tested in all environmental conditions.

Additionally, peel tests of two types of commercially available pressure-sensitive tapes with different backings (plastic and paper, respectively) were conducted on photographic print substrates for comparison. The tapes were Document Repair Tape, manufactured by Lyreco® and Sellotape®. Samples used in adhesive joints tests were subjected to post-fracture analysis, using optical microscopy and ESEM. This research also included a long-term natural ageing trial and a museum application case study.

[2] Due to limited access to samples or incompatibility of the materials with goals of this research, some of the samples considered could not be eventually examined. Authors would like to thank representatives of the institutions, materials from which could not have been included here, for their willingness to help and share insights into the technology and helping with preliminary assessment: Institut für Nueue Materialen (Germany), Phelsuma Inc. (USA), and nanoGriptech (USA).

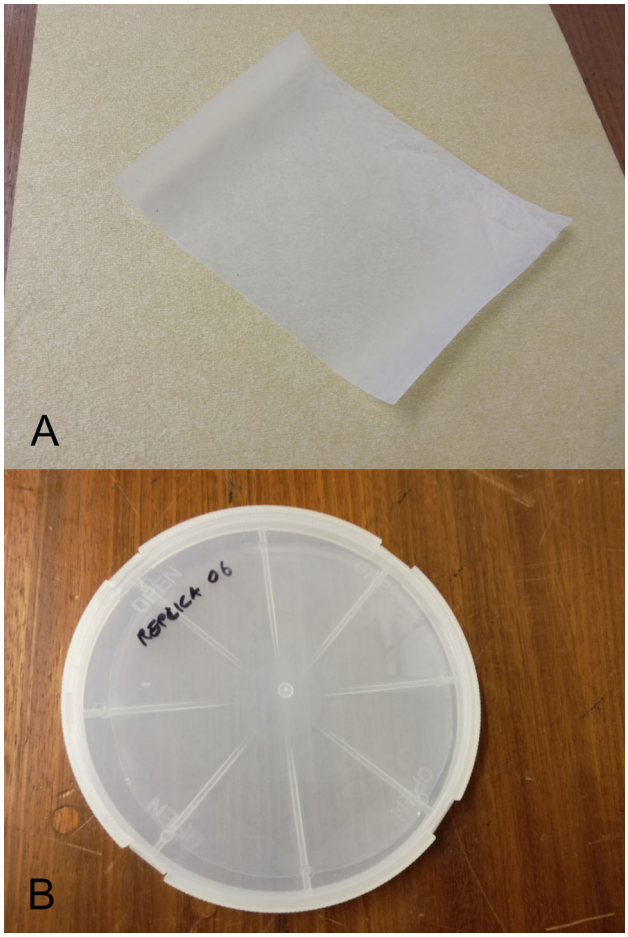

Fig. 3 GDAs in macroscale. **A** Fragment of the GB3 GDA tape, 10 cm wide; **B** Box with a round patch of the UOG2 GDA, 15 cm in diameter

Three types of GDAs acquired from the Gottlieb Binder GmbH were supplied as rolled strips, 10 cm wide and 1 m long. The first material, GB1,[3] was milky yellowish while the next two, GB2 and GB3 were colourless, almost transparent. Materials were supplied with release liners on both sides in the double-sided versions (GB2 and GB3) and on one side in the GB3 GDA. An example fragment of the GB3 material is shown in Fig. 3A. The three types of the GDAs supplied by Gottlieb Binder GmbH were: (1) first generation (since discontinued) of a double-layer GDA with a pressure-sensitive adhesive (PSA) as backing–marked here as GB1; (2) second generation of a double-layer GDA with a PSA backing–marked here as GB2; and a single-layer GDA, with no backing–marked here as GB3 (see Fig. 4A). Two more GDA types were prepared at the University of Glasgow: (1) thin sheets with 1cm^2 patches of adhesive areas (UOG1); and (2) thicker sheets fully covered in adhesive micropillars (UOG2; see Fig. 4B). Gelatine-based, colour and glossy photographic prints were ordered in a commercial photograph laboratory in London. The materials designed at the University of Glasgow (UOG GDAs) were delivered as round sheets of patterned transparent Polydimethysiloxane (PDMS). The first prototype (UOG1) was a round sheet, 5 cm in diameter, with square patches of pillared pattern, 1×1 cm each. The sheets were 0.9 mm thick. The second version of the Glasgow (UOG2) material was supplied as round sheets, each 15 cm in diameter, as shown in Fig. 3B, this material was between 1.5 and 3.1 mm thick. Two PSA tapes were bought from suppliers of stationery and office materials and colour photographic prints were ordered at a commercial photographic studio in London. Both tapes were bought in rolls 2.48 cm wide (1 inch). Photographic prints were ordered in 15×10 cm format with gloss finish on the recto (print) side.

Samples of each material were cut to size with utility knife at a ± 0.5 mm tolerance, between 24 and 48 hours prior to the test. All samples were kept in the set testing conditions for at least 24 hours before testing (up to 30 h). Joints were prepared immediately before testing to minimise contamination of sticky surfaces with dirt.

The protocol for mechanical testing of the joints was based on earlier stages of this research [23, 28]. The research presented here expanded relative humidity values in which the tests were conducted: 33%, 55%, and 75%. Similarly, the range of testing temperatures was increased: 5 °C, 21 °C, and 35 °C. This resulted in final set of nine testing environments (see Table 1). Tensile testing of photographic papers was conducted in all nine environments, while the GDAs were tested in tension in three temperatures, but only one RH. This decision was made because the polymers from which the GDAs were made of are hydrophobic, so the

[3] Shorthand codes were assigned by the authors and are not coming from any of the manufacturers.

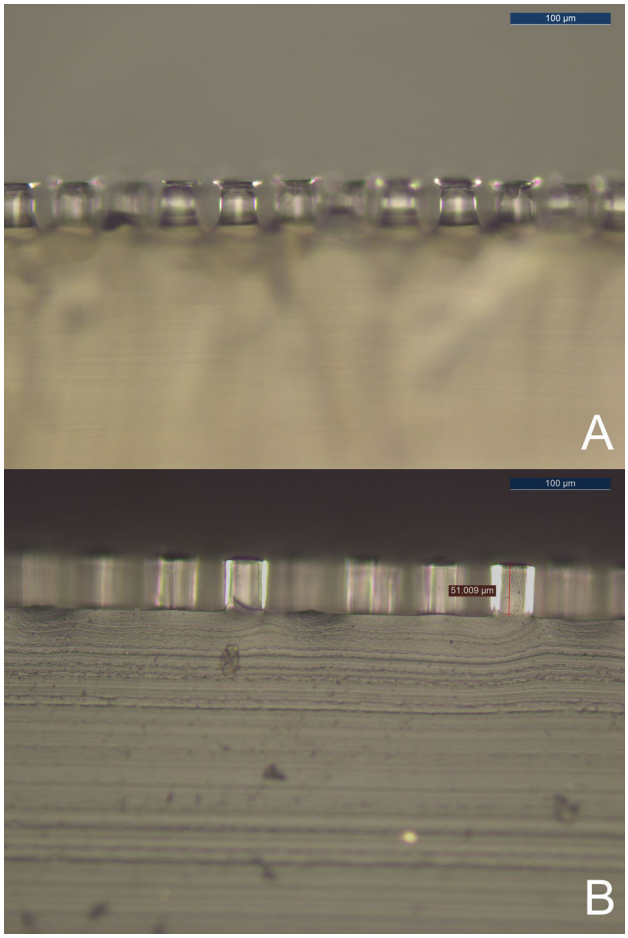

Fig. 4 Optical images of two types of the GDA micropillars. **A** GB2 GDA, micropillars with mushroom caps; **B** UOG2 GDA with straight cylindrical micropillars

influence of changes in relative humidity would be negligible. Sampling material was also hard to obtain. The joints were tested in shear and peel in all nine testing environments.

Joints tests were also used to conduct comparison peel tests in order to provide comparative values for the GDA adhesion. Samples of tape were attached to strips of photographic prints with just finger pressure, in the same way as in the GDAs tests. The tapes were left in ambient conditions for two weeks before peeling, in order to allow for the adhesive to bond properly [29, 30]. These peel tests were conducted in one set of environmental conditions–55% RH and 21 °C, with crosshead speed of 10 mm/min.[4] The DMA tests of the GDAs were conducted in film tension configuration with a temperature ramp, from − 150 °C to 35 °C, increasing at the rate of 3 °C/min. Tests were performed at 1 Hz and 10 Hz. Tan delta was calculated automatically by the software.

Mechanical tests were conducted with an Instron 4301 universal tester equipped with a 1 kN load cell and selected tests were later repeated as control with an Instron 5543 universal tester equipped with a 100 N load cell. Presented peel results have been smoothed to reduce the noise caused by the low resolution of the 1 kN load cell at low loads. Smoothing was achieved with local regression (rloess function) in MATLAB software. The resulting load-extension curve was fitted to start at (0,0) point. The average, minimum and maximum peel force of each sample was calculated between 30 and 60 mm of peel length. Statistical analysis of the results was conducted on the account of the influence of the testing environment (the main variable in the tests) on shear adhesion in the IBM Statistical Product and Service Solutions (SPSS) software.

4 Results

4.1 Material characterisation

All materials were imaged using optical microscopy and ESEM. All three generation of the GB GDAs showed the same pattern of micropillars: 50 µm in height, spaced approximately 50 µm (centre-to-centre) from each other, with rows shifted against each other,

[4] Tapes were tested in only one set of conditions because these tests were treated as supplementary and providing only ballpark numbers for comparison with the GDAs. However, environment-related changes in adhesive behaviour of PSA tapes have not been – to authors' best knowledge –as of yet tested.

Table 2 Basic dimensions of the GDAs tested. Data in microns. Codes as in Table 1

	GB1	GB2	GB3	UOG1	UOG2
Overall thickness	450	750	350	~900	~1500–3000
Gecko layer thickness w/o pillars	250	300	300	~850	~1850
Backing layer thickness	150	400	–	–	–
Pillars length	50	50	50	45	45
Pillars diameter w/o cap	20	20	20	45	45
Pillars cap diameter	30	30	30	–	–
Pillars spacing (centre-to-centre)	50	50	50	60–70	60–70

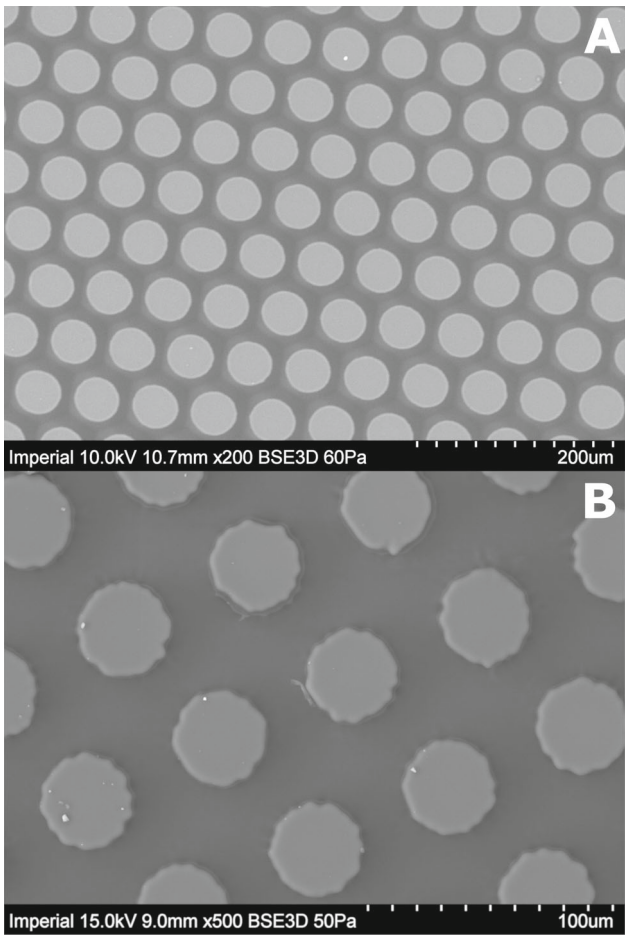

Fig. 5 ESEM images of the GDA micropillars arrays. **A** GB1 GDA array with mushroom caps; **B** UOG2 GDA cylindrical pillars

creating a rhomboidal lattice. The thickness of the shaft below the mushroom cap was estimated to be less than 20 μm. The cap takes approximately 10% of the micropillar's height and is approximately 30 μm wide (in diameter), as shown in Fig. 4. The difference between the three types of the GB material was the thickness of the PDMS under the micropillars and the thickness and colour of the backing layer in the two-sided materials (GB1 and GB2). The PDMS in the gecko layer of the GB1 material was 300 μm thick, and thickness of this layer increased to 350 μm in GB2 and GB3 GDAs (see Table 2 and Fig. 4). The colour of the PDMS layer has not changed at all. The backing colour has changed between the two types of bilayer GDA, from yellowish to colourless transparent.

The UOG2 GDA images showed micropillar structures on the surface of the PDMS layer. The micropillars on the surface of the PDMS had approximately cylindrical shape, with some irregularities in their cross-sectional outline and were slightly wider at the base than at the top. The micropillars had 45 μm in height and between 41 μm and 45 μm in diameter. The rows of micropillars were again shifted against each other, creating a rhomboidal lattice. This GDA did not have a regular lattice. In horizontal lines the pillars were spaced at 60 μm (centre-to-centre) and in diagonal lines they were spaced at 70 μm (centre-to-centre). ESEM images of both types of gecko pillars as shown in Fig. 5.

FTIR-ATR measurements were conducted to ascertain the polymers of the GB GDAs. Scans of the 'gecko' sides of the GB GDAs resulted in identical spectra on all three types of the GDAs. These spectra matched the reference spectra of PDMS films. In both GB GDAs that had PSA backing (GB1 and GB2), this adhesive was found to match polyurethane reference spectra (see

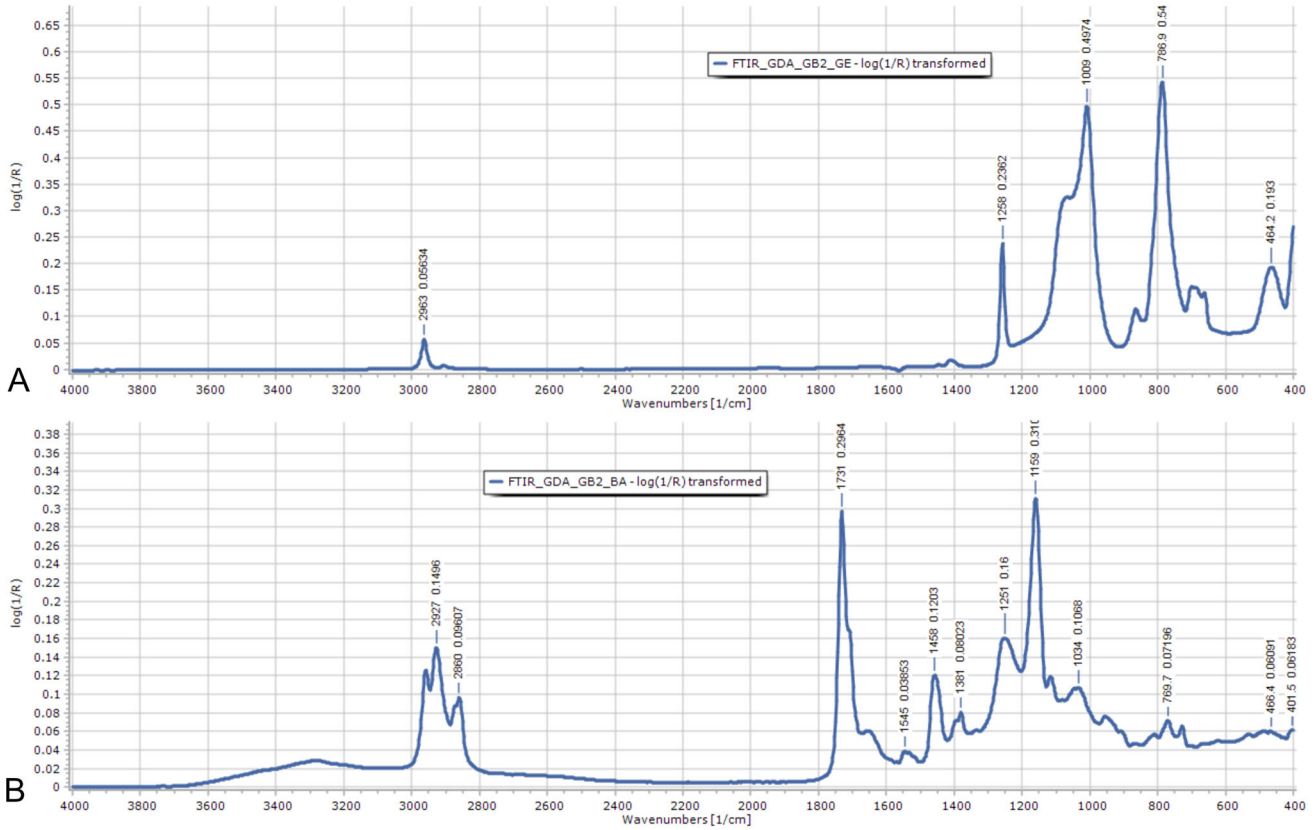

Fig. 6 FTIR spectra of two sides of the GB2 GDA. **A** Spectrum of the gecko layer matching PDMS pattern; **B** spectrum of the adhesive backing matching polyurethane pattern

Fig. 6). The FTIR-ATR on the UOG materials matched the PDMS reference spectra. The polymer used to make the UOG GDAs was known (Sylgard 184 PDMS elastomer by DOW Chemicals). Therefore, these FTIR results from the UOG GDAs could be used as references. The stationery adhesives tapes were also examined using FTIR-ATR. The scans of the Archival Tape revealed an adhesive based on polyurethane and the carrier based on cellulose (most likely wood pulp paper). The examination of Sellotape showed an adhesive layer made of polyurethane-based polymer (with spectrum almost identical to this of the Archival Tape) and a carrier made of polyethylene.

The GB1 GDA tests with DMA were conducted at 1 Hz, with two tan delta peaks measured at − 118 °C and − 18 °C. The other bilayer material, GB2 GDA was tested at 1 Hz and 10 Hz. Test resulted in two tan delta peaks at each frequency: at − 115 °C and at − 10 °C in the 1 Hz test, and at − 115 °C and at − 5 °C in the 10 Hz test. The UOG2 material was tested at 1 Hz, and only one tan delta peak was measure, at − 115 °C (see Fig. 7). Frequencies were selected as the most appropriate from previous research on glass transition temperature (Tg) in artistic and conservation materials [31].

Table 3 shows results of tensile tests conducted on GDAs at three temperatures and two RH levels.[5] Tensile samples were rectangular stripes, with a 70 mm gauge length between clamps. All samples were subjected to the same testing regime, with constant crosshead speed of 10 mm/min, and with maximum extension set at 50 mm. Maximum stress measured in GB1 GDA was 10.1 MPa ± 0.43 MPa at the maximum 0.71 tensile strain (equal to the preset maximum extension). All GB1 samples yielded at an average strain of 0.034 ± 0.003 and at an average stress of 5.74 MPa ± 0.20 MPa.

GB2 GDA reached overall average stress of 0.53 MPa ± 0.01 MPa at 0.71 strain. No sample had yielded. In GB3 GDAs maximum stress reached 0.91 MPa ± 0.04 MPa at 0.71 strain and none of the samples yielded within the boundaries of the testing parameters. The UOG samples, apart from one broke at the clamps of the instrument. Therefore, the results are less than ideally reliable. However, the one sample that broke at its centre did so at a 0.65 strain and at stress of 1.83 MPa.

Finally, stress relaxation tests were conducted on the GB2 and GB3 GDAs. Samples were prepared in the same way as the tensile tests samples and tensioned to 50 mm extension (0.71 strain) at 10 mm/min. The reduction in stress was recorded over time. GB2 sample lost 15% of its maximum stress after first 15 min, after which the stress plateaued, after 5 h the reduction in stress was 23%

[5] GB1 was tested earlier than other GDA types and the choice of preferred testing conditions was adjusted afterwards. However, this is not believed to have important influence on the results.

Table 3 Results of all the tensile tests conducted. Codes as in Table 1

Tensile test results		Relative humidity														
		33%					55%					75%				
			UTS avg [N]	UTS ± σ [N]	Max Stress avg [MPa]	Max Stress ± σ [MPa]		UTS avg [N]	UTS ± σ [N]	Max Stress avg [MPa]	Max Stress ± σ [MPa]		UTS avg [N]	UTS ± σ [N]	Max Stress avg [MPa]	Max Stress ± σ [MPa]
Temperature	5 °C	PH	273.10	11.32	68.20	3.13	GB2	8.06	0.31	0.56	0.02	PH	183.53	1.84	46.06	0.41
							GB3	4.97	0.25	0.92	0.04					
							PH	193.35	3.06	48.29	0.72					
	21 °C	PH	168.58	2.77	41.16	0.73	PH	169.56	4.02	42.41	0.99	PH	233.54	4.86	58.47	1.32
		GB1	77.70	2.78	10.12	0.43	GB2	7.04	0.30	0.48	0.02					
							GB3	4.85	0.14	0.88	0.03					
							UOG2	10.87	1.15	0.17	0.02					
	35 °C	PH	167.72	4.17	41.92	1.17	PH	218.70	5.57	54.60	1.43	PH	129.00	3.90	32.24	1.04
							GB2	7.87	0.15	0.55	0.01					
							GB3	5.14	0.10	0.94	0.02					

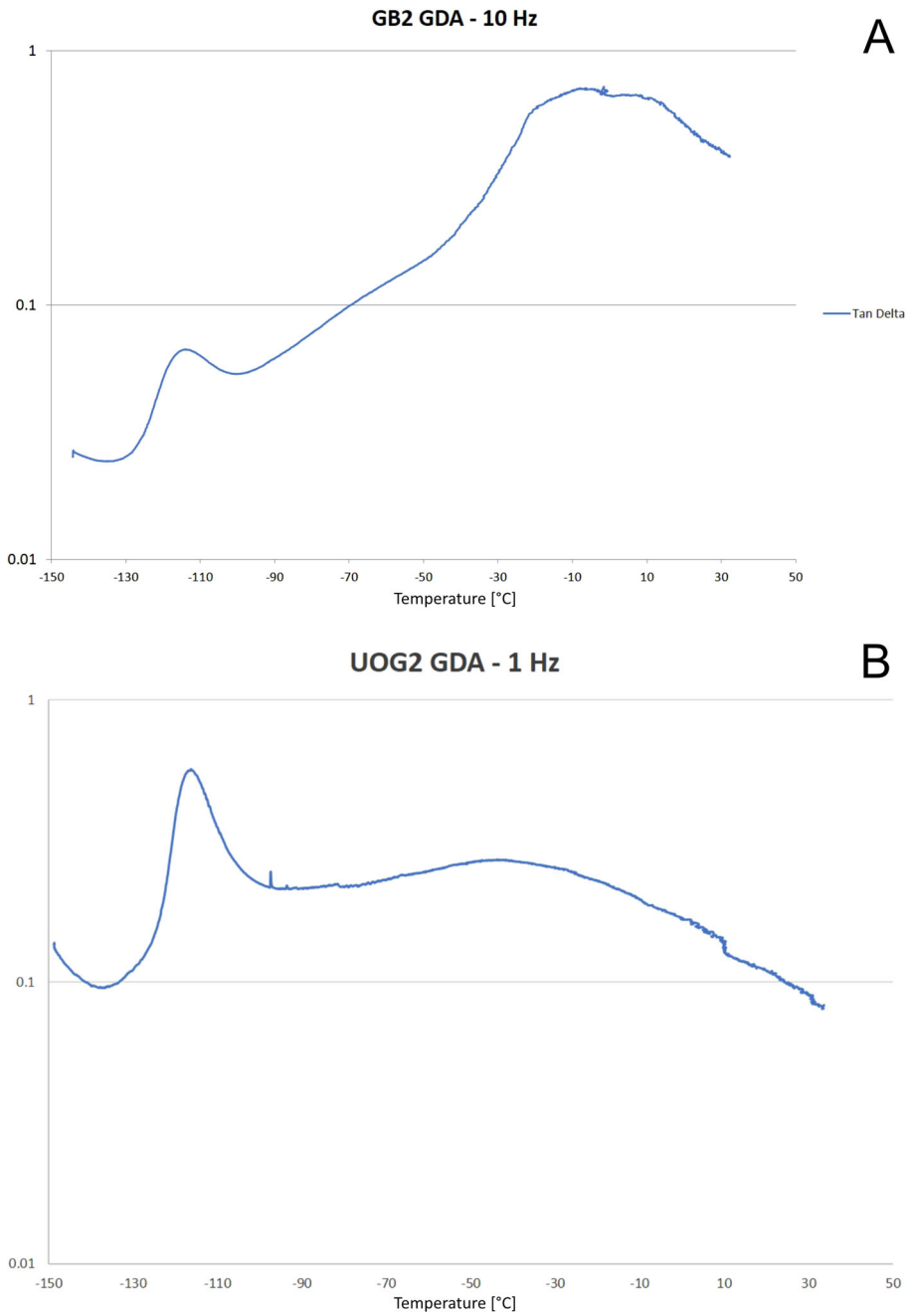

Fig. 7 DMA tan delta graphs of double- and single-layer GDA tapes. **A** Double-layer GB2 GDA with two peaks, one for PDMS at approx. − 115 °C and approx. − 10 °C; **B** Single-layer UOG2 with one peak at approx. − 115 °C

from the maximum value. GB3 GDA lost 17% of the maximum stress value after first 15 min, after which period the stress also plateaued. After 3 h the stress fell by 23% from the maximum value (see Fig. 8).

The photographic prints were characterised with optical microscopy, ESEM, FTIR-ATR and tensile testing. Both sides were imaged with optical and electron microscopes, and the cross sections were imaged under optical microscope in visible and UV light. The images showed a standard mass-produced photographic paper. Images of the recto showed a layer of transparent binder with coloured dots over a layer of white substrate, which can be assumed to be the photosensitive salts suspended in a layer of gelatine on polymer-coated paper. Images of the recto showed paper fibres coated with a layer of transparent resin. FTIR-ATR tests confirmed the standard composition of the prints, indicating gelatine as the binder on the recto side (characteristic peaks at 1536, 1632 and 3287 1 cm wavenumber) and polyethylene as the coating on the paper (characteristic peaks at 718, 1462, 2846 and 2914 1 cm wavenumber) from the verso side [32–35]. In tensile tests, prints samples were tested with the same parameters as the GDAs. All samples fractured during testing with an average calculated ultimate tensile strength of 407.9 MPa ± 7.3 MPa, at an average strain of 0.06 ± 0.02.

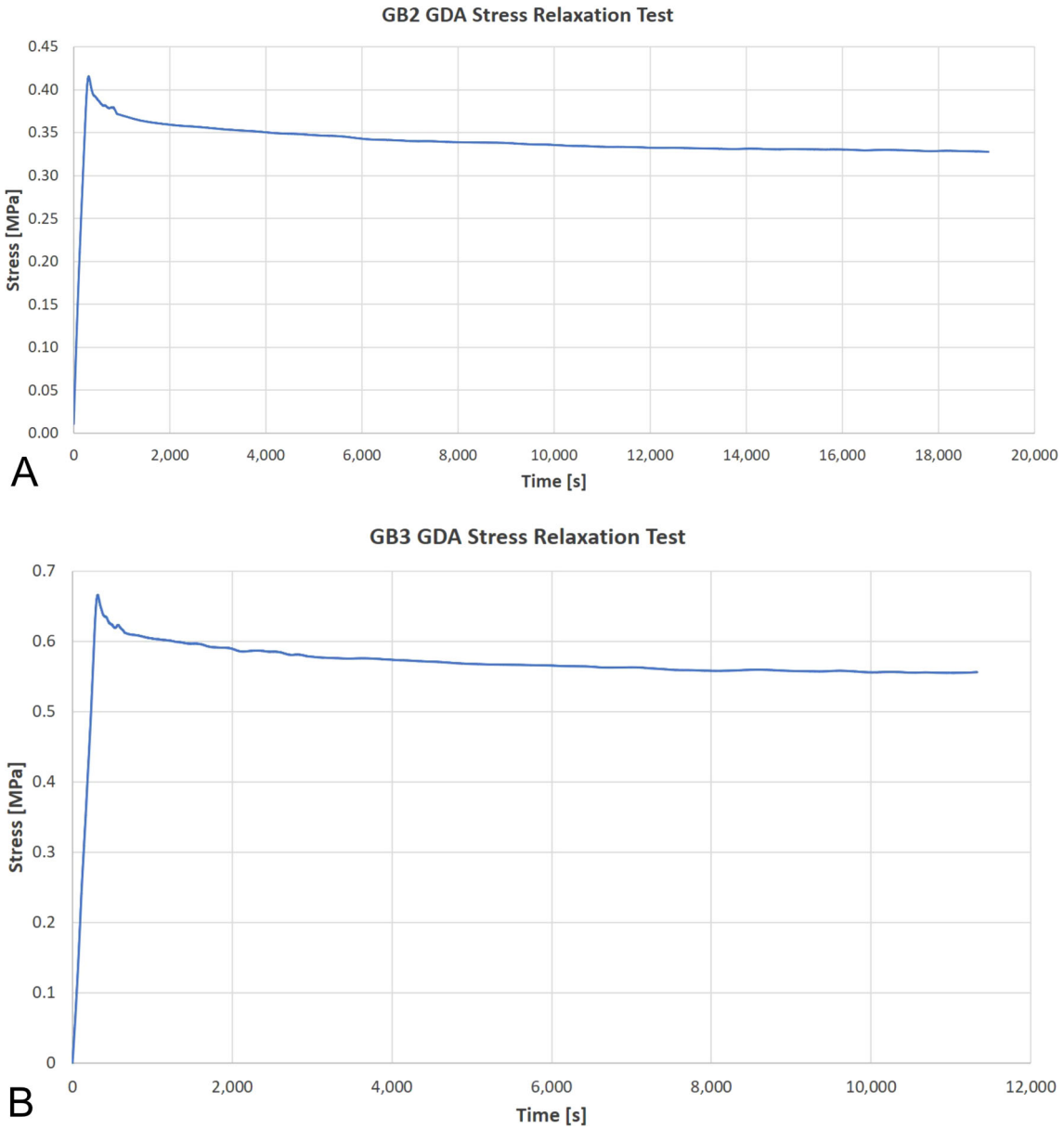

Fig. 8 Stress relaxation graphs showing strong early response and quick plateauing of the slope. **A** is the GB2 GDA graph and **B** is the GB3 GDA

4.2 Joints testing

The results from shear tests are shown in Table 4 and the results of peel tests are shown in Table 5. Each test was repeated five times for each environmental condition. Shear samples were prepared as a single lap joint with 8 cm^2 of overlap area (4×2 cm). T-peel strips were 2 cm wide and 7 cm long, with 2 cm on one side left for mounting the sample in the instrument clamps. All tests, both in shear and in peel, were conducted at a crosshead speed of 10 mm/min. The results are not given in Newton's per area or length because these GDA properties do not usually linearly change with size.[6] Thus presenting results normalised can be misleading without repeating the tests over a range of samples sizes.

[6] Due to its fibrillar structure, crack initiation and resulting detachment of GDAs occurs at the level of individual fibre tips. From this it can be assumed that the detachment process is dependent mostly on the resistance of individual fibres to crack initiation and their stiffness once a crack occurs at a weak spot. Each of these two factors is independent from the size of the GDA patch. And although a bigger patch can withstand larger shearing or pull-off forces due to the material working as one, once the crack initiation occurs at a weak spot, it spreads as quickly in each sample, and the size of the "buffer zone" in fibrillar adhesive is less important than in a continuous one. Furthermore, a larger sample has a higher probability to cover imperfections in the substrate surface that would serve as crack initiation spots.

Table 4 Results of all of the shear tests conducted. Codes as in Table 1

Shear test results	Relative humidity														
	33%					55%					75%				
		Fmax avg [N]	Fmax ± σ [N]	Fmax point avg [mm]	Fmax point ± σ [mm]		Fmax avg [N]	Fmax ± σ [N]	Fmax point avg [mm]	Fmax point ± σ [mm]		Fmax avg [N]	Fmax ± σ [N]	Fmax point avg [mm]	Fmax point ± σ [mm]
Temperature 5 °C	PH + GB2	10.55	0.49	39.44	2.85	PH + GB2	10.91	1.25	42.11	2.95	PH + GB2	11.04	1.68	43.23	4.30
	PH + GB3	9.24	0.48	49.67	0.30	PH + GB3	8.76	0.53	49.37	0.49	PH + GB3	8.90	0.29	49.37	0.88
21 °C	PH + GB1	48.09	2.68	1.64	0.21	PH + GB2	8.50	0.56	37.32	3.43	PH + GB2	8.19	0.85	32.46	3.46
	PH + GB2	8.86	0.68	34.40	2.91	PH + GB3	7.36	0.55	48.39	3.41	PH + GB3	7.31	0.82	43.61	4.99
	PH + GB3	8.50	0.62	48.39	2.12	PH + UOG1*	0.80	0.31	0.55	0.20					
						PH + UOG2	1.37	0.18	0.63	0.11					
35 °C	PH + GB2	10.43	0.54	41.57	2.33	PH + GB2	8.26	1.29	31.63	8.28	PH + GB2	6.89	0.13	27.89	2.24
	PH + GB3	6.17	0.54	40.27	3.15	PH + GB3	5.90	0.50	37.06	2.98	PH + GB3	7.95	1.75	46.48	5.90

*Results obtained from 1cm^2 samples

Table 5 Results of all the peel tests conducted

Peel test results		Relative humidity														
		33%					55%					75%				
		Sample	F avg [N]	F ± σ [N]	F min [N]	F max [N]	Sample	F avg [N]	F ± σ [N]	F min [N]	F max [N]	Sample	F avg [N]	F ± σ [N]	F min [N]	F max [N]
Temperature	5 °C	PH + GB2	0.38	0.11	0.14	0.61	PH + GB2	0.36	0.04	0.21	0.51	PH + GB2	0.42	0.04	0.26	0.59
		PH + GB3	0.31	0.10	0.00*	0.52	PH + GB3	0.20	0.10	0.28	0.54	PH + GB3	0.30	0.07	0.09	0.46
	21 °C	PH + GB1	0.30	0.06	0.10	0.44	PH + GB2	0.27	0.03	0.15	0.41	PH + GB2	0.28	0.06	0.04	0.44
		PH + GB2	0.28	0.06	0.12	0.50	PH + GB3	0.47	0.10	0.24	0.66	PH + GB3	0.22	0.04	0.07	0.38
		PH + GB3	0.24	0.07	0.00*	0.42	PH + UOG2	0.27	0.02	0.25	0.30					
							PH + TARC	4.07	0.45	2.86	5.10					
							PH + TSELL	1.14	0.14	0.77	1.45					
	35 °C	PH + GB2	0.40	0.17	0.18	0.80	PH + GB2	0.38	0.06	0.14	0.52	PH + GB2	0.37	0.06	0.20	0.51
		PH + GB3	0.23	0.05	0.04	0.40	PH + GB3	0.28	0.09	0.10	0.61	PH + GB3	0.27	0.10	0.02	0.69

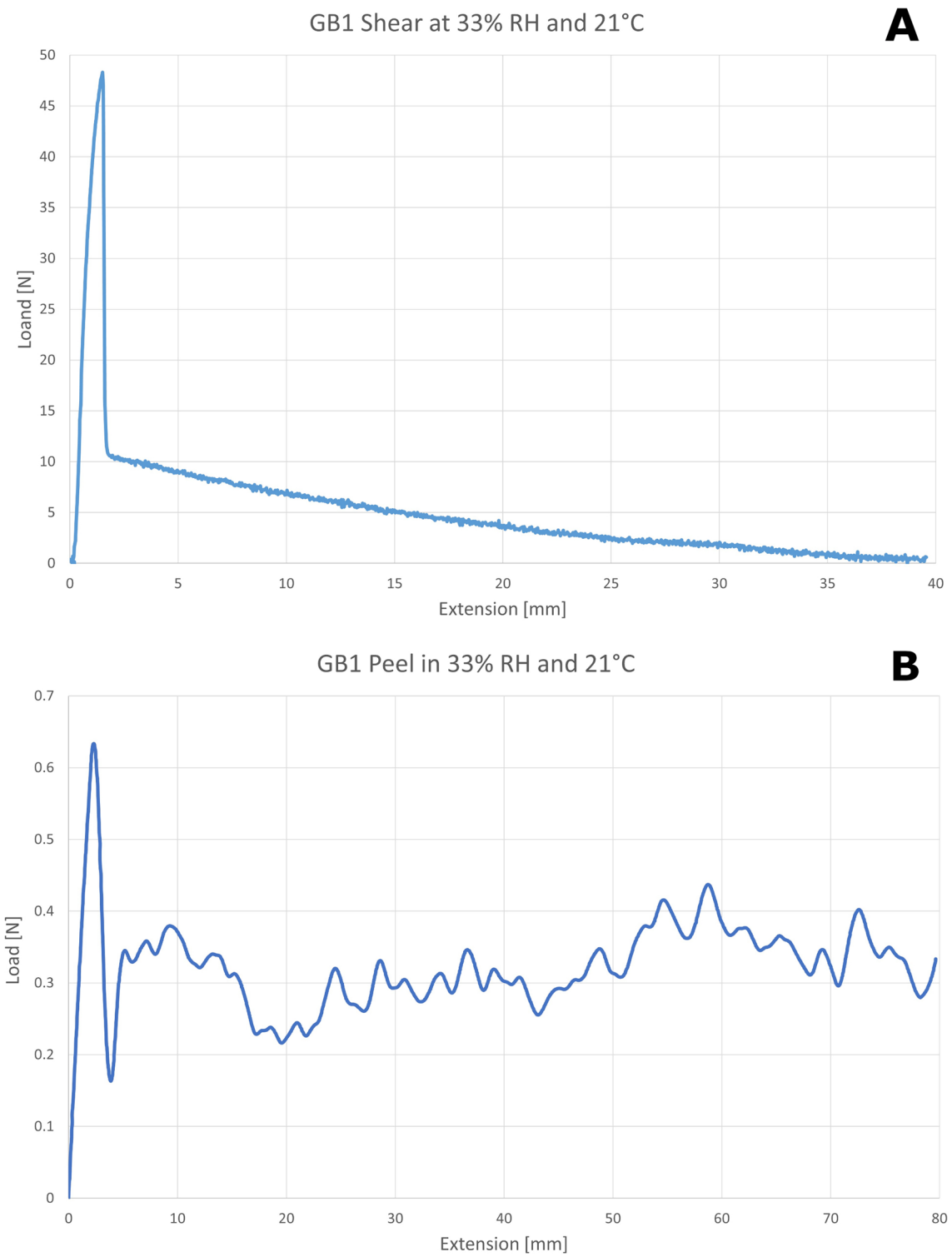

Fig. 9 Example graphs of load in testing of mechanical joints. **A** Shear test of the GB1 GDA. High load peak with following sliding visible. **B** GB1 GDA in peeling test. Initial peak was probably caused by the backing sticking to instrument clamps. Average load calculated from the section between 30 and 60 mm of extension

GB1 GDA was tested in peel and shear only at 21 °C and 33% RH. The average tensile shear force measured for five samples was 48.09 N ± 1.64 N at an average extension of 1.64 mm ± 0.21 mm. After that extension the force reduced but the GDA stayed connected to the photographic print and continued sliding along the substrate until extension exceeded the length of the joint overlap. The average peel force of the GB1 GDA was 0.30 ± 0.06 N (see Fig. 9 for example graphs).

GB2 GDA was tested in peel and shear in all nine environmental conditions (see Tables 4 and 5), each with 5 repeats. The mean maximum forces was calculated at 9.29 N ± 1.39 N, at a calculated average 36.67 mm ± 5.05 mm of extension. Shear force versus extension curves in all tests were similar, with a plateaux at the top of the curve, visually identified as being caused by the elastic extension of the GDA, predominantly in the area between the overlap part of the joint and the instrument grip. The lowest average shear force occurred at 35 °C and 75% RH and was 6.89 ± 0.13 N, while the highest average shear force was 11.04 ± 1.68 N, at 5 °C and 75% RH. In peel, GB2 material achieved overall force of 0.28 ± 0.08 N. The lowest average peel force occurred at 35 °C and 33% RH, 0.22 ± 0.05 N and the highest peel force of 0.42 ± 0.04 N occurred at 5 °C and 75% RH.

Similarly, GB3 GDA was also tested in nine environmental conditions, each with 5 repeats (see Tables 4 and 5). The average shear force was calculated at 7.79 N ± 1.12 N, at an average extension of 45.85 mm ± 4.29 mm. The curves of GB3 GDAs were flatter than the GB2. This was because the GDA contracted transversally (Poisson effect) after approx. 2 mm of extension, followed by the elastic deformation until the end of the test. The lowest average shear force of 5.90 ± 0.50 N occurred at 35 °C and 55% RH and the highest average shear force of 9.24 ± 0.48 N occurred at 5 °C and 33% RH. In peel, the lowest average force was 0.20 ± 0.10 N, at 5 °C and 55% RH and the highest average peel force was 0.47 ± 0.10 N, at 21 °C and 55% RH. The average peel force of all GB3 GDA samples was calculated at 0.28 ± 0.10 N.

The UOG1 and UOG2 GDAs were tested at 21 °C and 55% RH only, due to scarcity of the material. UOG1 GDA reached average shear force of 0.8 N ± 0.31 N, but from 1cm^2 overlap at an average extension of 0.55 mm ± 0.20 mm. This GDA has not detached after reaching maximum shear force, but it stayed connected and continued to slide along the substrate print with a pronounced ringing pattern, i.e. with the load cyclically falling and coming back up again, albeit to a slightly lower lever than in the cycle before. UOG2 reached an average shear force of 1.37 N ± 0.18 N, with maximum shear loads registered on average at 0.63 mm ± 0.11 mm. The connection had not broken in any of the samples but the GDA kept on sliding until reaching the end of the substrate. In the case of UOG2 shear tests, the ringing pattern was more pronounced. UOG1 samples, due to their size could not have been peeled off, as the stiffness of the PDMS prohibited such small patches to be stretched back without immediate springing away from the substrate. UOG2 samples were peeled in 21 °C and 55% RH, and their average peel force was 0.27 ± 0.02 N (see Tables 4 and 5).

Peeling of the PSA tapes was conducted only at one environmental condition of 21 °C and 55% RH. Sellotape reached average peel force of 1.13 ± 0.14 N, with peaks reaching 1.45 N. Archival tape reached average peel force 4.06 ± 0.44 N, with peaks reaching 5.10 N.

4.3 Long-term and in situ testing

As a form of separate, long-term testing, set of 10, 2 × 1 cm^2 patches of the GB1 GDA was attached to ten various surfaces around the conservation studios, where it remained in place for two years, exposed to changes in environmental conditions as well as ambient levels of dirt and light. Surfaces used as substrates included lacquered wood furniture, PVC-coated chipboard, PMMA glass, regular glass and acrylic house paint. Samples were not disturbed mechanically for the entire period but were visually checked every two months. After two years the materials were detached, photographed and attached back again for additional 24 h period in order to test whether they have lost their ability to stick after detachment (as usually occurs with most pressure-sensitive adhesives.

Finally, a short experiment in practical use of the material has been conducted at the Silesian Museum in Katowice, Poland. A small (outline measurements 25 × 50 × 20 mm, weight 12 g) polyester resin sculpture was immobilised in its exhibition showcase with a 1 cm^2 patch of the GB2 GDA (see Fig. 10). The sculpture had to be fixed to the glass pedestal on which it was placed, due to fear of a visitor accidently pushing the case and causing the sculpture to slide along the glass and damage. Both GB3, GB2 and UOG2 materials were tried for this application, but double-sided nature of the GB2 GDA was decisive in the choice of the material. The sculpture was attached directly to the PDMS gecko layer, while the PSA backing was adhered to the glass slate base inside the showcase. The GB2 GDA remained in this function for the entire length of the exhibition, which lasted just over three months. After deinstallation of the exhibition, the GDA patch that was used was examined with a colourimeter against a patch of the material that was kept in the museum, in the same conditions, but shielded against light.

4.4 Post-fracture analysis

After the adhesive tests, all samples were examined under 4× optical magnification. Samples showing possible damage were then examined with an optical stereomicroscope at magnifications between 5 and 50× and ESEM (magnifications 40–200×). No traces of residue or of mechanical damage were found on either the GDAs or the substrate photographs, only surface dirt on both sides of all materials was found and it was identified as a result of handling (see Fig. 11).

5 Discussion

Material characterisation revealed the key features of the GDAs. In all materials from Gottlieb Binder GmbH the FTIR examination suggests that the ‘gecko’ layers were made with Poly(dimethyl siloxane) or a very closely related polymer, with very probable presence of additives. This latter conclusion is drawn from the fact that the pure PDMS is transparent, and these GDA films are

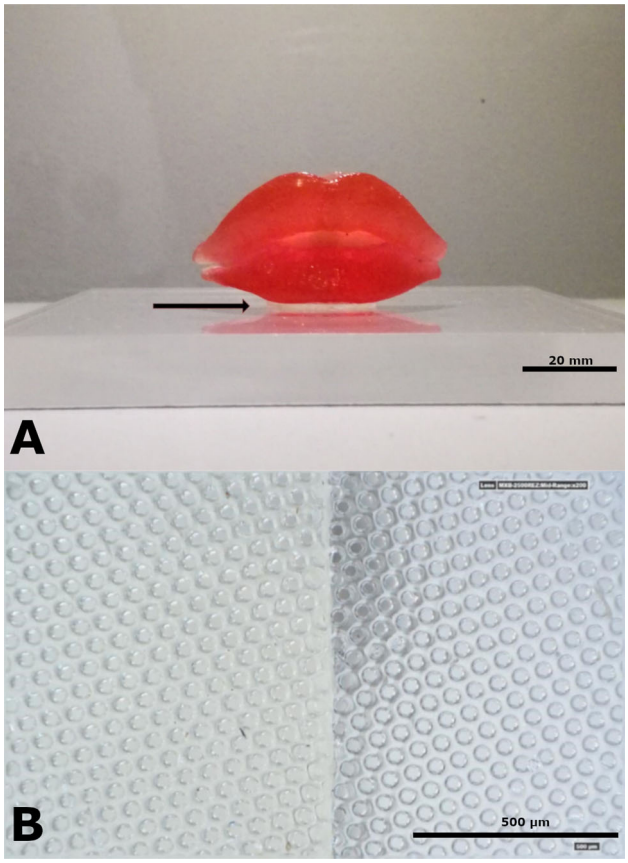

Fig. 10 Image of Szapocznikov's "Mouth" polyester sculpture with **A** GB2 GDA patch holding it in place (GDA marked by the arrow, width of the patch is 20 mm)). **B** Colourimetry with used GB2 GDA on the left and the unused sample on the right. Images by Małgorzata Momot. Sculpture from the collection of Dr Werner Jerke, presented at the "Perspective of Adolescence. Szapocznikow–Wróblewski–Wajda" Exhibition, at the Silesian Museum in Katowice, Poland

not. Microscope imaging confirmed the architecture of all of the GDAs and their dimensions. FTIR examination also showed that the pressure-sensitive backings of the double-layered GDAs were made of either polyurethane, or its copolymer, or a polymer very closely related to polyurethane. However, despite showing almost identical spectra under the FTIR-ATR examination, there is a stark difference in tensile strength between the two generations of the Gecko Nanoplast® bilayer GDAs (GB1 and GB2). This difference is likely to be a result of a change in composition or manufacturing of the backing material. However, more analytical research would be needed to fully explain the difference in the mechanical behaviour between these two materials. The unsuccessful attempt at conducting tensile tests on the UOG GDAs was not a big setback, because the exact polymer used for their manufacture was known and the data for its mechanical properties are available in literature [36]. Only one PDMS sample fractured in the centre at a strain of 0.65, with a peak stress of 1.83 MPa Calculated Young's modulus was 2.47 MPa, fitting closely data presented in [36] for PDMS cured at 150 °C [5, 28].

DMA examination showed that the polymers used have glass transitions temperatures firmly below zero, close to the literature data for the PU and PDMS: − 15 °C and − 125 °C, respectively. Both these polymers have melting temperatures significantly above the temperatures used this research: crosslinked PDMS stays stable until at least 300 °C and most of the PUs is stable until approx. 90 °C. Therefore, the polymers that make up the GDAs tested were firmly in the viscoelastic regions when being examined with tensile tests. Changes in testing temperature did not influence neither the ultimate tensile strength in any of the GDAs, nor any their elastic behaviour. This corresponds well with the DMA obtained and literature data for the polymers identified in the FTIR examination. Interestingly however, only one GDA, the GB1, showed any signs of plastic behaviour during testing, while all the other materials remained in their elastic regions within the testing parameters. It also showed much higher tensile strength than other GDAs within the testing strain. Changes in temperature and humidity did influence the behaviour of the photographic papers. Interestingly, temperature seemed to have more influence than RH on the behaviour of the prints. It can be speculated that this is caused by the polymer coatings on both sides of the paper that are there precisely for the purpose of minimising the effect of humidity ingress, yet they are responding to changes in temperature themselves.

Changes in RH and temperature did not significantly influence either the shear or the peel tests for any of the material pairings tested. There are some differences between various materials and their peel and shear forces, but no significant temperature or RH effect was found. In order to quantify the influence of testing environment on the shear adhesion, statistical analysis (anova) was conducted on the shear test results. As it is shown in Fig. 12A, B, in shear testing of GB2 material increase in RH had an impact on the performance of the adhesive-material system, while changes in temperature had negligible influence. It is suggested that this is caused by the changes in behaviour of the photographic prints rather than in the adhesive. In general, the overall stiffness of the

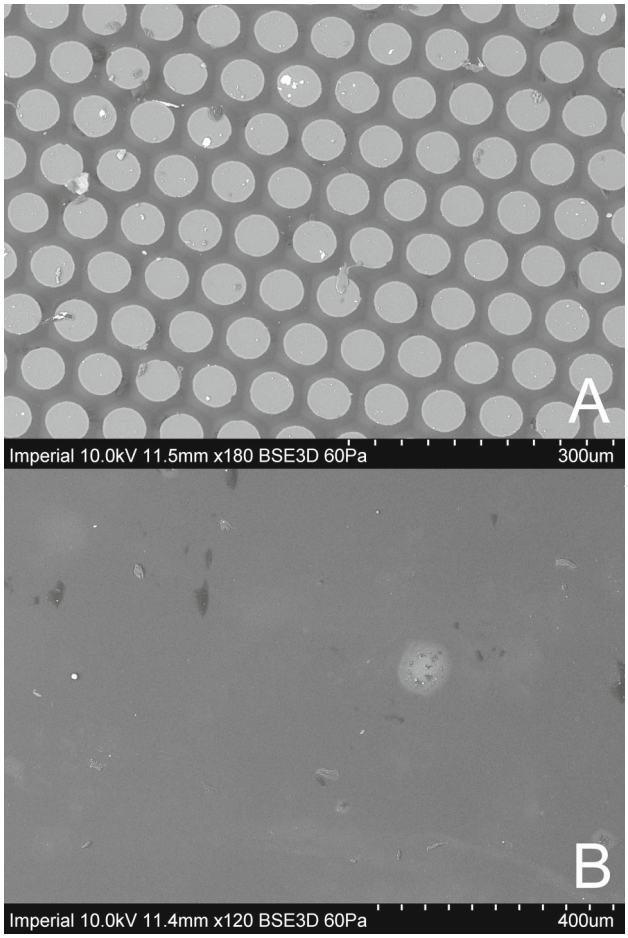

Fig. 11 ESEM Post-fracture images. They show no mechanical damages, only dirt. **A** GB2 GDA and **B** surface of the photographic paper

entire system is crucial for effectiveness of the GDA shear adhesion, as it prevents peeling from occurring. Because of the low peel strength, bending of the system that changes the geometry towards peeling, or the Poisson effect to occur, will increase chances of system failure. Similar results were identified in analysis of the GB3 shear tests. However, as it can be seen in Fig. 12C, D, changes in temperature did cause a fall in shear adhesion, but only in the batches tested in 75% RH. Reasons behind this are unclear. One explanation is that in 75% RH the overall increased elasticity of the system strengthens other factors weakening the joint. However that result is not consistent with the tensile testing of photographic papers as individual materials, and as such it requires further investigation.

It has been shown that the commercial GDA with mushroom caps on the tips of its micropillars had better performance than the custom-made UOG GDA with micropillars with straight tips. In shear tests GB GDAs have shown over $4\times$ higher strength (comparing the lowest GB GDA shear strength with the UOG GDA), while keeping very similar levels of peel strength. This comparison offers a key insight into two problems of the GDAs. Firstly, the GDA adhesion does not scale up linearly. The results achieved with 8 cm^2 lap joints were 58% higher than the results achieved from the 1 cm^2 overlap (1.37 N versus 0.8 N). Secondly, there probably is influence of the overall thickness of the GDA material. It is possible that some if not all of the difference between the increase of the joint's overlap area and the increase in the shear strength of the joint described above was caused by the greater thickness of the UOG2 GDA. The thickness of the UOG2 material could cause a shift of the pulling axis during shear testing what as a result would introduce a bending moment. What in turn would turn detachment into peeling process, speeding up the failure of the joint.

GDAs have been shown to fulfil the key promise of the technology: the properties of high adhesive shear strength with very low peel. Especially when the peel for the GDAs are compared with the commercially available PSA tapes. Peel forces registered in GDAs were over 50% lower than these of PSA tapes, even if the highest result of a GDA is compared with the lowest result of a PSA peel test. Sellotape peeled at an average force of 1.13 ± 0.14 N from the 2 cm wide sample, while the highest peel force registered in all GDA tests was 0.47 ± 0.10 N from 2 cm peel front (GB3 GDA in 21 °C and 55% RH). This means the potential for incurring damage is much lower for the GDAs than for the PSA tapes, with better reversibility. The composition and physical properties of the backing layer in the GDA material have significant impact on the overall performance of the GDA, comparable to the impact of the mushroom caps on the tips of the micropillars. The GDA with the highest stiffness (GB1) had over $4\times$ higher shear strength

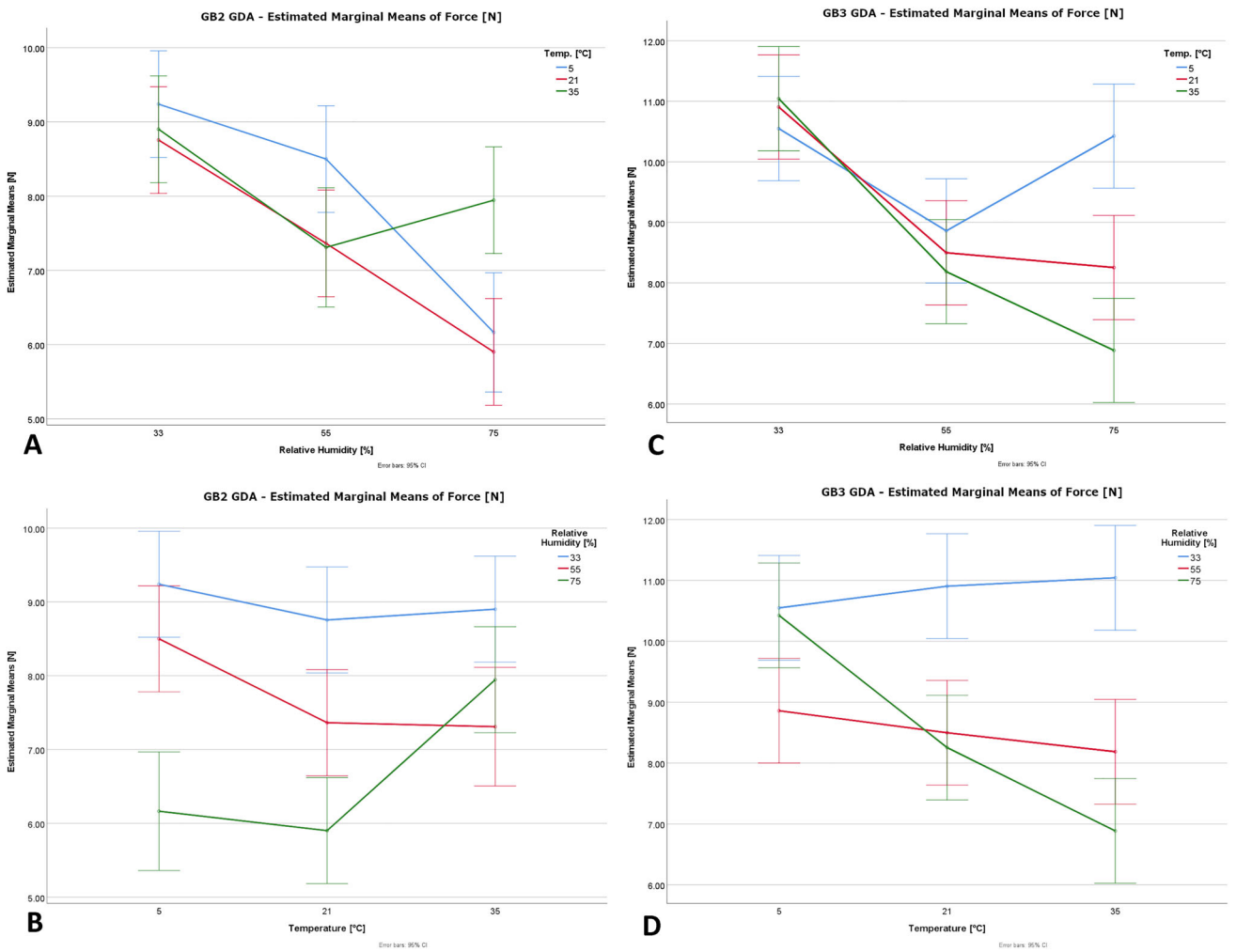

Fig. 12 Parametric graph showing the results of Anova analysis on the results of GB2 (graphs A and B) and GB3 (graphs C and D) GDAs shear testing. **A** and **C** graphs comparing influence of change in RH on batches tested in a given temperature; **B** and **D** graphs comparing influence of change in temperature on batches tested in a given RH

than the second best-performing GDA (GB2 GDA in 5 °C and 75% RH). The elastic modulus for the GB1 GDA was calculated to be 0.23 GPa, while the elastic modulus of the GB2 GDA was calculated to be 0.0008 GPa. This correlation partially corroborates the results obtained by Bartlett et al. [37], who have tested soft, viscoelastic polymers without fibrillar structures. In their research they suggested that a soft adhesive layer with backing which is linearly stiff in the shearing direction offers the strongest adhesion in that shearing direction.

The GB1 GDA in the long-term ageing test remained attached without any naturally occurring detachment between the gecko layer and any of the substrates it was attached to. In the reattachment test at the end of the 2 years period the GDA samples remained as capable of adhering to the same substrates as two years prior. They remained in place for another 24 hours without detaching. Samples examined under an optical microscope, 5–50 × magnification, show no obvious changes to their GDA layer. However, the PSA backing had yellowed significantly and started detaching from the gecko layer, as well as collecting significant amount of dust (see Fig. 13). There was also dust observed around the GDA patch on the substrate surfaces that just settled there. Presumed presence of chemical modifiers or additives in the PDMS layer is a potential issue in long-term use of the GDAs. However, the gecko layer in the GDA tested has not visibly aged over the two-years test and did not lose its elasticity as estimated by eye and touch. The PSA backings containing polyurethane are a more urgent issue, potentially mitigated by the availability of single-layer GDAs.

In the museum showcase experiment, after the end of the exhibition the GB2 GDA and the object it was securing were examined under an optical microscope (20 × magnification). The sculpture showed no visible changes and no traces of the adhesive on its surface, unfortunately this inspection was not documented. Further analysis was not possible due to time constraints, but it would be advisable in the future. The GDA, however, showed some change in colour. The change was identified as coming from the pressure-sensitive backing. The change in colour was measured with a colourimeter, comparing with another GB2 GDA patch that was stored in dark, cold place for the same period. Measurement conducted in the L*a*b space showed Delta $E = 3.16$, a visible difference in

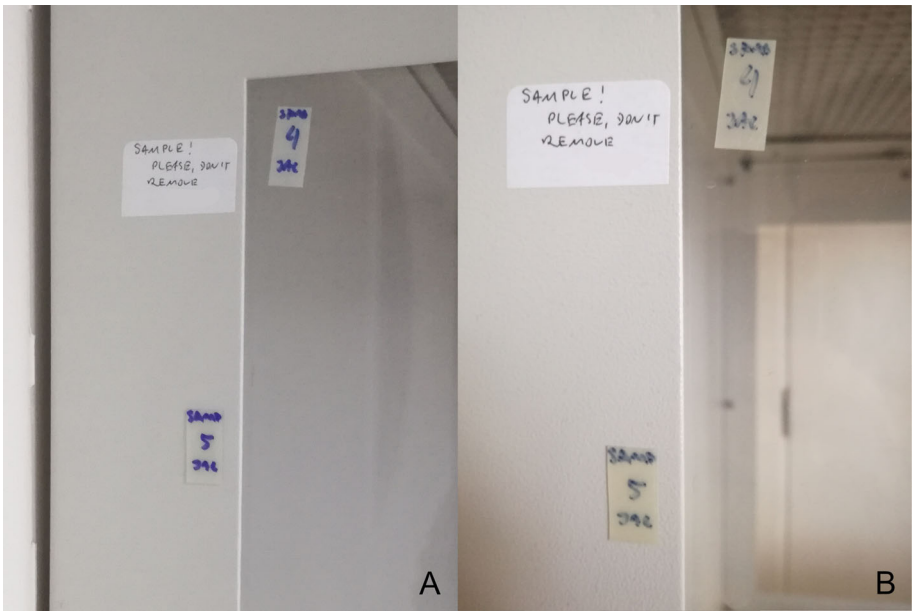

Fig. 13 GB1 GDA samples left in open laboratory space (on the side of a fume hood). **A** Just after attachment and **B** after 2 years

colour, identifiable with naked eye (see Fig. 10B). The case study showed no adverse effects of the GDA in the showcase, as the object was insulated from direct contact with the polyurethane layer by the PDMS layer. Because of that the main danger coming from the polyurethane decomposition is off-gassing. It was not tested in this research so its influence remains a potential problem for future research.

Following the proposed flow chart steps allowed to assess the performance of a new adhesive technology and its potential application in conservation. The last step of the flow chart, H—Feedback, in this research is the importance of understanding the overall composite structure of the adhesive. The potential new areas for investigation include the importance of the stiffness and thickness of the entire GDA composite, as well as the geometry of the micropillar tips. On the other hand, it has been shown that the GDAs can easily perform in a wide range of temperatures and relative humidity without significantly losing their strength. The key importance of the flow chart is highlighting the need to test of the entire adhesive-substrate material systems. Only this kind of research into adhesive behaviour within the system makes it possible to establish the safety margins for a new technology.

6 Conclusions

This project has demonstrated that GDAs do have a strong potential for applications in heritage conservation. So far, their range of potential use is limited to smooth surfaces [5]. However, there are significant advantages of using the GDAs. When a substrate is receptive to GDA adhesion, then the GDA will stick to it potentially indefinitely. The effective lifetime is limited only by eventual decomposition of the PDMS, which is a polymer of considerable chemical stability. It was confirmed that a GDA adheres immediately with full strength under only gentle finger pressure.[7] The anisotropic behaviour of the GDAs has been confirmed, and the peeling was shown to be significantly easier, requiring far less force than breaking the connection in the shear direction.

In the future, the surface properties of the potential substrates which affect the capability of the GDAs to adhere should be investigated. This would facilitate the design of materials with wider applications in the field of heritage conservation. Additionally, a range of composite backings should be tested in order to allow for better tailoring of the properties of the adhesive. For example, the lowering of the GDAs Poisson's ratio should in turn result in materials capable of sustaining greater loads in shearing. GDAs have proven useful in a short-period application in an in situ test. More controlled tests are necessary to definitively declare GDAs as safe, but currently it can be assumed that short- and mid-term applications (several months of continuous use) are fully within reach of the state-of-the-art technology.

Acknowledgements Authors would like to thank Dr Ruth Brooker from Imperial College London and Dr Cecilia Gauvin for their help in setting up some of the experiments. Thanks for help in conducting the museum experiment go to Małgorzata Momot, MA, paper conservator at the Silesian Museum in Katowice, Poland. Additionally, authors would like to thank Dr Ambrose Taylor and Prof. Anthony Kinlock from Imperial College London, Dr Paul Messier from Yale University, and Pierce Townshend, independent paper conservator for providing insightful comments regarding some of the initial research questions and following results. Thanks for help with statistical analysis are due to Dr Maciej Kosiło. The development of the testing protocol was possible thanks to discussions with curatorial and collection management teams at The Hunterian, University of Glasgow. Experimental work was supported by a

[7] In-line with previous research on the same topic we define finger pressure at approx. 15 N/cm^2 [5].

scholarship from The Courtauld Institute, London and parts of the final data analysis were supported by a postdoctoral fellowship project "Gecko-inspired dry adhesives for packing, transport and display in museum collections" funded by the AXA Research Fund.

Data Availability Statement Detailed data of each sample tested are available upon request from the Authors. This manuscript has associated data in a data repository. [Authors' comment: Detailed data for each sample tested are available upon request from the Authors.].

References

1. K. Wanieck, P.-E. Fayemi, N. Maranzana, C. Zollfrank, S. Jacobs, Biomimetics and its tools, bioinspired. Biomim. Nanobiomaterials. **6**, 53–66 (2017). https://doi.org/10.1680/jbibn.16.00010
2. P.E. Fayemi, K. Waniek, C. Zollfrank, N. Maranzana, A. Aoussat, Biomimetics: process, tools and practice. Bioinspir. Biomim. **12**, 0110022 (2017). https://doi.org/10.1088/1748-3190/12/1/011002
3. G. Marom, The biomimetic evolution of composite materials: from straw bricks to engineering structures and nanocomposites. J. Compos. Sci. **5**, 123 (2021). https://doi.org/10.3390/jcs5050123
4. J.F.V. Vincent, O.A. Bogatyreva, N.R. Bogatyrev, A. Bowyer, A.-K. Pahl, Biomimetics: its practice and theory. J. R. Soc. Interface. **3**, 471–482 (2006). https://doi.org/10.1098/rsif.2006.0127
5. J. Olender, J. Perris, Y. Xu, C. Young, D.M. Mulvihill, N. Gadegaard, Gecko-inspired dry adhesives for heritage conservation–tackling the surface roughness with empirical testing and finite element modelling. J. Adhes. Sci. Technol. (2022). https://doi.org/10.1080/01694243.2022.206115
6. M. Storari, F. Di Lorenzo, B. Cattaneo, M. Collina, G. De Cesare, M. Ioele, N. Macro, A.R. Rubino, M. Torre, "Vortice e Figura" di Paola Levi Montalcini: intervento su u n'opera polimaterica con supporti footografici affetti da sindrome acetica, in: XVII Congr. Naz. IGIIC – Lo Stato Dell'Arte – Chiesa Di Cris. Flagellato Dell'ex Osp. San Rocco, Matera, 10–12 Ottobre 2019, Matera, 2019: pp. 111–120.
7. V. Horie, *Materials for Conservation: Organic Consolidants, Adhesives and Coatings*, 2nd edn. (Routledge, London, 2011)
8. B. Appelbaum, *Conservation Treatment Methodology* (Butterworth-Heinemann, Oxford, 2007)
9. S. Muñoz Viñas, Minimal Intrevention Revisited, in *Conserv. Princ. Dilemmas Uncomfortable Truths*. ed. by A. Richmond, A. Bracker (Butterworth-Heinemann, Oxford, 2009), pp.47–59
10. H. Aristotle, *History of Animals* (Clarendon Press, Oxford, 1910)
11. K. Autumn, Y.A. Liang, S.T. Hsieh, W. Zesch, W.P. Chan, T.W. Kenny, R. Fearing, R.J. Full, Adhesive force of a single gecko foot-hair. Nature **405**, 681–685 (2000). https://doi.org/10.1038/35015073
12. J.B. Puthoff, M. Holbrook, M.J. Wilkinson, K. Jin, N.S. Pesika, K. Autumn, Dynamic friction in natural and synthetic gecko setal arrays. Soft Matter **9**, 4855 (2013). https://doi.org/10.1039/c3sm50267h
13. K. Autumn, A. Dittmore, D. Santos, M. Spenko, M.R. Cutkosky, Frictional adhesion: a new angle on gecko attachment. J. Exp. Biol. **209**, 3569–3579 (2006). https://doi.org/10.1242/jeb.02486
14. G. Huber, S.N. Gorb, N. Hosoda, R. Spolenak, E. Arzt, Influence of surface roughness on gecko adhesion. Acta Biomater. **3**, 607–610 (2007). https://doi.org/10.1016/j.actbio.2007.01.007
15. A.Y. Stark, T.W. Sullivan, P.H. Niewiarowski, The effect of surface water and wetting on gecko adhesion. J. Exp. Biol. **215**, 3080–3086 (2012). https://doi.org/10.1242/jeb.070912
16. H. Izadi, K.M.E. Stewart, A. Penlidis, Role of contact electrification and electrostatic interactions in gecko adhesion. J. R. Soc. Interface. **11**, 20140371–20140371 (2014). https://doi.org/10.1098/rsif.2014.0371
17. P.H. Niewiarowski, S. Lopez, L. Ge, E. Hagan, A. Dhinojwala, Sticky gecko feet: the role of temperature and humidity. PLoS One. **3**, e2192 (2008). https://doi.org/10.1371/journal.pone.0002192
18. S. Hu, S. Lopez, P.H. Niewiarowski, Z. Xia, Dynamic self-cleaning in gecko setae via digital hyperextension. J. R. Soc. Interface. **9**, 2781–2790 (2012). https://doi.org/10.1098/rsif.2012.0108
19. A.K. Geim, S.V. Dubonos, I.V. Grigorieva, K.S. Novoselov, A.A. Zhukov, S.Y. Shapoval, Microfabricated adhesive mimicking gecko foot-hair. Nat. Mater. **2**, 461–463 (2003). https://doi.org/10.1038/nmat917
20. M. Sitti, R.S. Fearing, Synthetic gecko foot-hair micro/nano-structures as dry adhesives. J. Adhes. Sci. Technol. **17**(2003), 1055–1074 (2014). https://doi.org/10.1163/156856103322113788
21. E. Arzt, H. Quan, R.M. McMeeking, R. Hensel, Functional surface microstructures inspired by nature–From adhesion and wetting principles to sustainable new devices. Prog. Mater. Sci. **120**, 100823 (2021). https://doi.org/10.1016/j.pmatsci.2021.100823
22. J. Fenn, Adhesion Without Adhesives: Gecko-Like Adhesives, in *CCI Symp*. (Adhes. Consolidants Conserv Res Appl. Canadian Conservation Institute, Ottawa, 2011)
23. J. Olender, C. Young, A. Taylor, The Applicability of Gecko-Inspired Dry Adhesives to the Conservation of Photographic Prints, in *ICOM-CC 18th Trienn. Conf. Prepr. Copenhagen, 4–8 Sept 2017*. ed. by J. Bridgland (International Council of Museums, Paris, 2017), p.0913
24. H. Izadi, N. Dogra, F. Perreault, C. Schwarz, S. Simon, T.K. Vanderlick, Removal of particulate contamination from solid surfaces using polymeric micropillars. ACS Appl. Mater. Interfaces. **8**, 16967–16978 (2016). https://doi.org/10.1021/acsami.5b09154
25. D.E. Packham (ed.), *Handbook of Adhesion*, 2nd edn. (John Wiley & Sons, Chichester, 2005)
26. S. Ebnesajjad, A.H. Landrock, *Adhesives Technology Handbook*, 3rd edn. (William Andrew, London, 2015)
27. W. Brockmann, P.L. Geiß, J. Klingen, S. Bernhard, *Adhesive Bonding: Materials* (Wiley-VCH Verlag GmbH, Weinheim, Applications and Technology, 2009)
28. J. Olender, Gecko-inspired Dry Adhesives: Evaluating their Applicability to the Conservation of Cultural Heritage, Courtauld Institute of Art, 2019.
29. I. Benedek, *Pressure Sensitive Adhesives and Applications*, 2nd edn. (Marcel Dekker Inc., New York, 2004)
30. D.W. Aubrey, Pressure-sesnsitive Adhesives–Adhesion Properties, in *Handb Adhes*, 2nd edn., ed. by D.E. Packham (Wiley, Chichester, 2005), pp.365–368
31. C. Young, *The Glass Transition Temperature of Adhesives – Preliminary Guidelines for Canvas Painting Treatments* (Archetype Publications, London, 2011). https://doi.org/10.1007/s13398-014-0173-7.2

32. V. Rouchon, E. Pellizzi, K. Janssens, FTIR techniques applied to the detection of gelatine in paper artifacts: from macroscopic to microscopic approach. Appl. Phys. A. **100**, 663–669 (2010). https://doi.org/10.1007/s00339-010-5649-5
33. J. Hossan, M.A. Gafur, M.R. Kadir, M. Mainul, Preparation and characterization of gelatin-hydroxyapatite composite for bone tissue engineering. Int. J. Eng. Technol. IJET-IJENS. **14**, 24–32 (2014)
34. B. Sarker, D.G. Papageorgiou, R. Silva, T. Zehnder, F. Gul-E-Noor, M. Bertmer, J. Kaschta, K. Chrissafis, R. Detsch, A.R. Boccaccini, Fabrication of alginate-gelatin crosslinked hydrogel microcapsules and evaluation of the microstructure and physico-chemical properties. J. Mater. Chem. B. **2**, 1470–1482 (2014). https://doi.org/10.1039/c3tb21509a
35. J.V. Gulmine, P.R. Janissek, H.M. Heise, L. Akcelrud, Polyethylene characterization by FTIR. Polym. Test. **21**, 557–563 (2002). https://doi.org/10.1016/S0142-9418(01)00124-6
36. I.D. Johnston, D.K. McCluskey, C.K.L. Tan, M.C. Tracey, Mechanical characterization of bulk Sylgard 184 for microfluidics and microengineering. J. Micromech. Microeng. **24**, 035017 (2014). https://doi.org/10.1088/0960-1317/24/3/035017
37. M.D. Bartlett, A.B. Croll, D.R. King, B.M. Paret, D.J. Irschick, A.J. Crosby, Looking beyond fibrillar features to scale gecko-like adhesion. Adv. Mater. **24**, 1078–1083 (2012). https://doi.org/10.1002/adma.201104191